Effect of porogen solvent on the synthesis of nickel ion imprinted polymer materials prepared by inverse suspension polymerization

Meouche, Walid

2017-02

Meouche , W , Laatikainen , K , Margaillan , A , Silvonen , T , Siren , H , Sainio , T , Beurroies , I , Denoyel , R & Branger , C 2017 , ' Effect of porogen solvent on the synthesis of nickel ion imprinted polymer materials prepared by inverse suspension polymerization ' , European Polymer Journal , vol. 87 , pp. 124-135 . https://doi.org/10.1016/j.eurpolymj.2016.12.022

http://hdl.handle.net/10138/310027
https://doi.org/10.1016/j.eurpolymj.2016.12.022

acceptedVersion

Effect of porogen solvent on the synthesis of nickel ion imprinted polymer materials prepared by inverse suspension polymerization

Walid Meouche[a,1], Katri Laatikainen[b], André Margaillan[a], Timka Silvonen[b], Heli Siren[c], Tuomo Sainio[b], Isabelle Beurroies[d], Renaud Denoyel[d], Catherine Branger[a*]

[a] Université de Toulon, MAPIEM, EA 4323, 83957 La Garde, France.

[b] Lappeenranta University of Technology, Laboratory of Industrial Chemistry, P.O. Box 20, FI-53851 Lappeenranta, Finland.

[c] University of Helsinki, Department of Chemistry, Laboratory of Analytical Chemistry, PO Box 55 (A.I. Virtasen aukio 1), FI-00014 University of Helsinki, Finland

[d] Aix-Marseille Université, CNRS, MADIREL UMR 7246, 13397 Marseille Cedex 20, France.

ABSTRACT :

Ion-imprinted polymers (IIPs) for nickel were synthesized by inverse suspension copolymerization of vinylbenzyl iminodiacetic acid (VbIDA) with ethyleneglycol dimethacrylate (EDMA) in presence of nickel(II) ions. They were prepared with mixtures of DMSO and acetonitrile, 50/50 %v/v, for IIP-A/D and DMSO and 2-

* Corresponding author.
Tel : +33-4-9414-6729 Fax : +33-4-9414-2448 E-mail address : branger@univ-tln.fr (C.Branger)
[1] Present address: Modern Univeristy for Business and Science, School of Health Sciences, Damour, Near Mechref Entrance. Lebanon.

methoxyethanol, 50/50 %v/v, for IIP-M/D. The structure and properties of these polymers were compared with those of IIP-D previously prepared with pure DMSO as porogen solvent. Although IIP-A/D and IIP-M/D were less porous than IIP-D, they presented better nickel adsorption properties and selectivity towards Zn^{2+}, Co^{2+} and Pb^{2+}. This is assumed to be the result of the stabilization of the ligand-metal complex during the polymerization process. The impact of the VbIDA chelating monomer was highlighted by comparing the adsorption properties of a copolymer of methyl methacrylate (MMA) and EDMA with NIP-D. It was proved that the methacrylic polymer matrix has low binding properties. Finally, a comparative study with Amberlite® IRC 748, a commercial chelating resins with IDA groups proved that selectivity of IIPs toward nickel is coming from an imprinting effect and not from the choice of the chelating functions. Moreover, the nickel binding capacities of the prepared IIPs in competitive conditions are remarkably high (184 µmol/g for IIP-D, 170 µmol/g for IIP-A/D and 174 µmol/g for IIP-M/D) compared to that of Amberlite® IRC 748 (315 µmol/g).

Keywords: ion-imprinted polymer, inverse suspension polymerization, porogen, nickel

1. Introduction

Because of its natural presence in the earth crust and its large consumption in the industry (refining, electroplating, and welding), pollution of the environment by nickel has become an unavoidable concern. The presence of nickel in water is due to direct leaching from rocks and sediments [1]. Nickel is responsible for various pathologies such as skin allergies, lung fibrosis, variable degrees of kidney and cardiovascular

system poisoning, stimulation of neoplastic transformation and cancer of the respiratory tract [1,2]. Moreover, all nickel compounds, except the metallic form, have been classified as carcinogenic to humans [3]. For these reasons, there is a constant need for the extraction and quantification of nickel, as well as of most of heavy metals.

Solid-phase extraction is widely used either for decontamination or preconcentration before a quantification step. For metal ions, it is currently based on ion-exchange or chelating sorbents [4,5]. These materials proved to be very efficient, with large adsorption capacities, good mechanical properties and reusability. Nevertheless, they are not adapted if selectivity is desired, for instance to recover a metallic compound. Selective extraction of metal ions from aqueous solutions can be successfully achieved using ion-imprinted polymers (IIPs) [6,7]. These polymers are prepared in the presence of an ion playing the role of a template in order to create binding cavities after its removal. The rigidity of the polymer network and the stability of the recognition cavities are provided by a high crosslinking rate. Chelating or ion-exchange functions are usually introduced in the form of a functional comonomer. This can be some classical commercial monomer such as acrylamide [8], acrylic acid [9] or 4-vinylpyridine [10,11] or home-made monomers based on ligands such as benzo-15-crown-5-acrylamide [12], N-methacryloyl-(L)-histidine [13,14] or vinylbenzyl 2-(aminomethyl)-pyridine [15].

In order to favor the interactions with the liquid phase and to make the binding cavities accessible, imprinted polymers need to be porous materials. This is the reason why a solvent called “porogen” solvent is always used even when “bulk” polymerization is implemented. The role of this porogen agent for the elaboration of porous polymers has been intensively studied and is mainly related to its thermodynamic affinity with the

monomers and the copolymer [16,17]. As far as imprinted polymers are concerned, the polarity of the porogen impacts the level of interactions between the template and the functional monomer. It is thus usually chosen in order to promote these interactions and therefore aprotic and low polar solvents are usually preferred [18,19]. However for IIPs, the first requisite for the porogen, which is to dissolve the monomers, the initiator and the template, can imply the use of protic and/or polar solvents because of the nature of the functional monomer and of the ion template. Although the impact of the porogen is well known, only few systematic studies have been carried out. Gladis and Rao used different porogens to synthesize IIPs for uranyl: 2-methoxyethanol, methanol, tetrahydrofuran (THF), acetic acid, dichloroethane, N,N-dimethylformamide (DMF) and toluene [20]. They showed that the selectivity varied with the polarity of the solvent with the best capacity and selectivity obtained with 2-methoxyethanol. More recently, Godlewska-Zylkiewicz et al. compared the performances of Pd(II)-IIPs prepared with chloroform, cyclohexanol and ethanol [21]. They concluded that the porogen did not significantly influence the analytical properties of the sorbent and they advise the application of polar porogen in case the IIP is planned to be used for the separation of analyte from aqueous samples.

In a previous work, we described a new route to synthesize IIPs in a bead format by inverse suspension polymerization [22]. IIPs for nickel were thus prepared with vinylbenzyl iminodiacetic acid (VbIDA) as the functional monomer. The very polar DMSO solvent was used to allow phase separation of the dispersed polymerization medium from the continuous non polar phase. The present paper describes a follow-up of this preliminary work in which we study the role of the porogen on the IIPs properties. Moreover, the impact of interfering cations (Co^{2+}, Zn^{2+} and Pb^{2+}) on the

adsorption kinetics of nickel was followed over a period of 24 hours. Finally, a comparison was done with two reference materials: (i) a copolymer of methyl methacrylate (MMA) and ethyleneglycol dimethacrylate (EDMA) to evaluate the influence of the methacrylic polymer backbone and (ii) the commercial iminodiacetic acid (IDA) bearing Amberlite® IRC 748 to study the imprinting effect.

2. Experimental

2.1. Materials

Vinylbenzylchloride (90% technical grade), iminodiacetic acid (IDA), ethylene glycol dimethacrylate (EDMA) (98% technical grade), 2-methoxyethanol were used as received from Acros Organics. Dimethylsulfoxide (DMSO) and acetonitirle were used as received from Fischer Scientific (99% technical grade). Mineral oil (d = 0.862), azobis(isobutyronitrile) (AIBN), nickel(II) nitrate hexahydrate (99.9%, $Ni(NO3)_2.6H_2O$), cobalt(II) nitrate hexahydrate (>98%, $Co(NO3)_2.6H_2O$), zinc(II) nitrate hexahydrate (>99%, $Zn(NO_3)_2.6H_2O$), lead(II) nitrate hexahydrate (>99%, $Pb(NO_3)_2.6H_2O$), calcium nitrate tetrahydrate (>99%, $Ca(NO_3)_2.4H_2O$), tris(hydroxymethyl)aminomethane (TRIS) and 4-(2-pyridylazo) resorcinol (PAR) were used as received from Sigma Aldrich.

2.2. Instrumentation

FTIR spectroscopy was performed in transmission mode on KBr pellets (32 scans, resolution 4 cm^{-1}) on a Nicolet Nexus apparatus. Nitrogen adsorption–desorption isotherms at 77 K were determined with a Micrometrics ASAP2010 apparatus. Before the adsorption experiment the samples were evacuated several hours at a pressure lower than 10^{-3} Pa and a temperature of 50 ºC. Scanning electron microscopy (SEM) images

were taken using a Philips XL30 microscope. A Shimadzu UV-2501 PC was used for absorbance measurements with one centimeter matched quartz cells. pH measurements were performed with a digital pH meter (Hanna Instruments, model HI 92240). Metal ion concentrations were determined by plasma emission spectroscopy (Iris Intrepid II XDL ICP-AES). All samples were analyzed at least twice and the duplicate determinations agreed within variation of 5%. The detection limit of the compounds with plasma emission spectroscopy was 0.1 mg/L.

2.3. IIPs synthesis by inverse suspension polymerization

The ionic imprinted polymers (IIPs) and non-imprinted polymers (NIPs) copolymers were prepared according to our previous work [22]. For the preparation of IIPs, the organic phase was prepared by dissolving VbIDA and $Ni(NO_3)_2.6H_2O$ with the following proportion 315 mg/175mg in 8 mL of the porogen solvents (composition given in Table 1). After 45 min of continuous stirring, 3 mL of EDMA and 10 mg of AIBN were added and the solution was stirred for 30 min under argon. Polymerization was carried out in a 250 mL round-bottomed flask with reflux condenser. 80 mL of mineral oil were placed in the flask and purged with argon. The organic phase was then added dropwise. The polymerization reaction was run at 80 °C for 4 h under mechanical agitation (500 rpm) and argon purging. The resin beads were collected by filtration and extracted in a Soxhlet 24 h with a chloroform–acetone mixture (1:1). They were then dried under vacuum for 24 h at room temperature. Non-imprinted polymers (NIPs) beads were prepared and treated in the same manner without nickel.

2.4. Poly(MMA-co-EDMA) synthesis

The copolymer of MMA and EDMA, poly(MMA-*co*-EDMA) was prepared using a similar protocol to that described earlier. The organic phase was prepared by dissolving MMA and EDMA (weight % w:w - 10:90) in 8 mL of DMSO. The rest of the procedure remained unchanged.

2.5. Nickel adsorption measurements

The resins were equilibrated at pH 7.5 and dried in vacuum at 60 ^{o}C. After equilibrium the nickel retention properties were determined by immersing 10 mg of dried resin beads in 10 mL of a nickel solution during 24 h under orbital agitation (60 rpm). The pH has been maintained at 7.5 during the experiment by using a sodium hydroxide solution (1 mol.L^{-1}). The remaining nickel concentrations in the solution were measured by UV–Vis spectroscopy by adding a buffer solution of TRIS (2 mol.L^{-1}) and HCl (1 mol.L^{-1}) (pH 8.0) containing PAR colorimetric agent (7.10−5 mol.L^{-1}). PAR can form an orange complex allowing the determination of nickel concentration at 495 nm.

2.6. Selectivity experiments

Selectivity and uptake kinetics of NIPs, IIPs, poly(MMA-co-EDMA) commercial Amberlite® IRC 748 were studied in mixed metal solution with metal concentrations of 20 mg/L Ni, Co, Pb and Zn in nitrate media. All measurements were made at room temperature, at constant pH = 7.5, and at a constant supporting ionic strength I_s = 0.1 mol/L adjusted with KNO_3. Before selectivity and uptake kinetic experiments, polymers were equilibrated at pH 7.5 and dried in vacuum at 60^{o}C. Equilibration time was one week. After equilibration, 1 g dry polymer was weighted into each mixed metal solution batch (V_{tot} = 1 L) with constant rotary mixer (mixing rate = 250 rpm) and samples (10 mL) were taken after 10 min, 1 h, 2 h, 4 h, 8 h, 24 h, and 48 h by keeping pH at 7.5

during the experiment. The bound amounts of each metal were calculated from the initial and equilibrium solution concentrations analyzed by ICP-AES.

The effect of calcium and magnesium to competitive binding of nickel, cobalt, lead and zinc was studied similarly, except 50 mg polymer was weighed in glass vials containing mixed metal solution with concentrations 20 mg/L nickel, cobalt, lead and zinc and 100 mg/L magnesium and calcium. The liquid volume of all samples was 50 mL. The samples were shaken at room temperature by keeping pH at 7.5 during the experiment. The bound amounts of each metal were calculated from the initial and equilibrium solution concentrations analyzed by ICP.

Selectivity coefficients, *k*, for binding of specific metal ion in presence of competitor specie can be obtained from adsorption data according to Equation (1) [23].

$$k = \frac{K_d(template\ ion)}{K_d\ (interfering\ ion)} \qquad \text{Equation (1)}$$

where: $K_d = \frac{Q_e}{C_e}$ is the distribution coefficient of an ion between the polymer and the solution

The effect of ion imprinting on selectivity was studied with relative selectivity coefficient, *k´*, as defined in Equation (2) [23].

$$k' = \frac{(k)_{\mathrm{IIP}}}{(k)_{\mathrm{NIP}}} \qquad \text{Equation (2)}$$

where k_{IIP} and k_{NIP} are the selectivity coefficients of imprinted and non-imprinted polymers, respectively.

3. Results and Discussion

3.1. Synthesis and textural characterization of IIPs and NIPs

IIPs and their corresponding non-imprinted polymers (NIPs) were prepared via inverse suspension polymerization as previously described [22]. In this earlier work, mineral oil was used as the continuous phase and DMSO as the porogen solvent. Changing the porogen solvent required to respect non miscibility with mineral oil and to allow solubilization of the VbIDA monomer. Because of these criteria, only acetonitrile and 2-methoxyethanol could be used as co-solvents, mixed with 50% in volume of DMSO. VbIDA monomer was introduced in a 10% w/w ratio as previously determined to be the optimum ratio.

FTIR spectroscopy was used to characterize the IIPs and NIPs and more specifically the leaching procedure of the nickel template (Figure 1). Distinctive bands of the poly(EDMA) backbone could be observed on all polymers spectra: the typical and intense C=O and C-O ester stretching bands at 1728 cm^{-1} and 1130 cm^{-1} respectively. The $–OCH_2$ deformation vibration band of EDMA was also present at 1460 cm^{-1} and the 1646 cm^{-1} band was characteristic from pendant vinyl CH_2=CH remaining groups. On the NIPs spectra, a band of the VbIDA monomer could be identified at 1560 cm^{-1} corresponding to the aromatic C=C stretching vibration. The C=O stretching band of the carboxylic acids functions could be observed at 1739 cm^{-1} as a shoulder on the EDMA ester C=O major band. On the contrary, for IIPs that still contained nickel ions (before any leaching procedure), this shoulder was no more observable and was replaced by strong asymmetric and symmetric $–CO_2^-$ stretching bands at 1604 and 1446 cm^{-1} respectively. These two bands disappeared upon acidic treatment of the IIPs and the high similarity of the leached IIPs and corresponding NIPs proved the efficiency of the acidic leaching treatment.

SEM observation revealed that independent particles could be obtained with average sizes in the range of 800 µm to 1 mm (Figure 2). However, while NIPs particles were almost spherical, IIPs presented more irregular shapes and surfaces. Porosity was studied by nitrogen adsorption/desorption experiments. All isotherms are of type IV indicating that all polymers are mainly mesoporous (Figure 3) [24]. The hysteresis loops show roughly parallel branches for NIP-D and NIP-M/D. They are close to the H1 hysteresis loop observed for sorbents with a narrow distribution of independent pores. In the case of all IIPs and NIP-A/D, the hysteresis loop is rather of H2 type. The adsorption and desorption curves are not parallel revealing a more complex structure with the presence of interconnected pores or of bottle-neck pores. It is worth noticing that for all IIPs and NIP10D2 an inflexion point is observed on the adsorption branch at relative pressure higher than 0.8, whereas the desorption occurs lower than 0.5 which may indicates large pores or cavities connected to outside by small openings leading to the phenomenon of desorption by cavitation. Consequently the pore size determined by applying the BJH method to the desorption branch may be inaccurate and gives only the highest possible value for these pore openings and it is possible to estimate the inside cavity sizes by applying the calculation to the adsorption branch. Table 1 presents surface areas determined by using the BET equation, average pore diameters calculated using the BJH model applied to the adsorption branch and microporous volumes from t-plot. As previously observed with DMSO, NIPs presented larger surface areas and porous volumes than the corresponding IIPs [22]. This could be due to strong interactions between VbIDA and nickel during the polymerization of IIPs. The introduction of a co-solvent to DMSO induced a decrease of porosity for the IIPs and an enlargement of the pores distributions. This was in accordance with the influence of the

diluent during the polymerization process which is known to impact the final porosity of the polymer material. If the solvent used as a porogen has a good affinity for the monomers and the copolymer, the phase separation will be late resulting in materials with large surface area [25]. The compatibility between the porogen and the monomers can be predicted by the solubility parameters (δ_i), using Hildebrand theory. Thus, the solvating power of the diluent is favored when $\Delta\delta^2 = (\delta_1-\delta_2)^2$ is minimized [17]. Solubility parameters for the different solvents DMSO, acetonitrile and 2-methoxyethanol are respectively: 19.2, 24.3 and 23.3 $MPa^{1/2}$ [26]. The solubility parameter of poly(EDMA) (19.2 $MPa^{1/2}$ [17]), representing 90% of the monomers, is closer to that of DMSO than of acetonitrile and 2-methoxyethanol and VbIDA was observed to be much more soluble in DMSO also. Thus the introduction of acetonitrile and 2-methoxyethanol as co-solvents with a ratio of 50% should induce a slight decrease of the polymers porosity, as observed in this study.

3.2. Adsorption of nickel and cross-selectivity kinetic study

In a first step, adsorption of nickel by the different resins was studied by batch experiments after an equilibration time of 24 hours (Figure 4). As expected, the affinity of IIPs for nickel(II) ions was always higher than that of NIPs as a result of the imprinting effect. The use of acetonitrile and 2-methoxyethanol as co-solvents induced an important rise of the IIPs maximum adsorption capacities (Table 1). In the same manner, imprinting factors for IIP-A/D and IIP-M/D were almost 50% superior to that of IIP-D. These results might not be directly linked to the porous structures of the polymers since IIP-A/D and NIP-A/D and IIPM/D are less porous than IIP-D and NIP-D. It is more likely that the polarity of acetonitrile and 2-methoxyethanol as well as the

protic character of 2-methoxyethanol are responsible for these results. Indeed, relative permittivities of DMSO, acetonitrile and 2-methoxyethanol are respectively 47.24, 36.64 and 17.2 [27]. So the introduction of acetonitrile and even more of 2-methoxyethanol decreases the polarity of the porogen mixture thus favoring the interactions between nickel and VbIDA. However, in the case of 2-methoxyethanol, its protic character might lower this effect and can explain the similarity of results between IIP-A/D and IIP-M/D. To conclude this study, it is also noteworthy that IIPs maximum adsorption capacities, varying from 14.2 mg/g to 23.9 mg/g, are in the upper range of values reported in the literature [28–31].

The cross-selectivity of resins towards divalent interfering cations (cobalt, zinc and lead) was studied over a large time scale running from 5 minutes to 24 hours (Figure 5). It clearly appeared that, initially -during the first 3 hours of contact- only IIP-A/D presented some selectivity towards nickel(II) ions. After that period, all the IIPs retained more nickel(II) than other cations and a plateau was reached after approximately 8 hours. As expected, for NIPs, no selectivity could be observed.

In order to determine the mechanism responsible for the adsorption process in these competitive conditions, the first order and second order kinetic models were applied - Equations (1) and (2) respectively.

$$ln\left[1-(1-\alpha)\frac{Q_t}{Q_e}\right] = -k_1\, t \qquad \text{Equation (1)}$$

$$\frac{t}{Q_t} = \frac{(1-\alpha)^2}{k_2\, Q_e^2} + (1-\alpha)\,\frac{t}{Q_e} \qquad \text{Equation (2)}$$

where Q_t and Q_e were the amount of the considered ion adsorbed at time t and equilibrium time respectively, expressed in µmol/g, α was the ratio between the concentration of the considered ion at equilibrium and at initial time and k_1 and k_2 were respectively the first and second order rate constants, expressed in min^{-1} and

g.µmol.min^{-1}. Table 2 summarizes the obtained results. Experimental data could not be fitted by the second order kinetic model, proving that chemisorption is not the limiting adsorption process of ions by the polymers [32,33]. The first order kinetic model, which assumes that the adsorption rate is proportional to the departure from equilibrium, could be successfully applied to nickel(II), zinc(II) and cobalt(II) adsorption but not to lead(II) ions. Comparison of k_1 values for nickel(II) and zinc(II) or cobalt(II) proved that nickel was retained more quickly than the other ions, especially by the IIPs. Nevertheless, the rate constants were low implying a long contact time required to obtain saturation ($t_{1/2}$, calculated as $\ln 2/k_1$, were between 2.6 and 3.1 hours) so this precludes the use of these IIPs for online applications.

Adsorption capacities, determined at equilibrium (t = 24h) in those competitive conditions, were higher for the IIPs than for the corresponding NIPs as an evidence of the imprinting effect (Table 3). The cross-selectivity results were in accordance with the retention of nickel alone: the use of a fraction of acetonitrile or 2-methoxyethanol with DMSO noticeably improved the selectivity of IIPs as can be evidenced by the values of relative selectivity coefficients. The imprinting effect was even most discernible in the case of competition with lead(II).

3.3. Comparison with reference materials

A reference copolymer was prepared replacing VbIDA by MMA as a comonomer with a view to study the impact of the ligand on the adsorption properties. MMA was chosen because its chemical structure was very close to that of EDMA and thus should not induce different interactions that this crosslinker does with the studied ions. Synthesis of

poly(MMA-*co*-EDMA) was performed with DMSO as porogen solvent in the same conditions as NIP-D (VbIDA replaced by 10% w/w of MMA).

The nitrogen adsorption/desorption isotherms of poly(MMA-*co*-EDMA) compared to that of NIP-D proves that… (Isa, Renaud : pouvez-vous m'aider à compléter ce §, svp ?; s'il n'y a rien de particulier à dire on se contente de mettre la surface spé et on ne met pas la fig 6). Peut-on conclure que même si SBET est plus faible pour le poly(MMA-*co*-EDMA), elle reste suffisamment importante et pas trop différente de celle du NIP-D pour que les résultats puissent être comparés ?

The adsorption of nickel(II) by the poly(MMA-*co*-EDMA) resin was studied in batch conditions after 24h of contact to be compared with that of NIP-D. A plateau was reached very quickly for an initial concentration of 3 mg/L of nickel with a maximum adsorption capacity of only 32 µmol/g. This value was significantly lower than the capacity of NIP-D (139 µmol/g) and evidenced the low impact of the methacrylic matrix on the retention of nickel. A cross-selectivity study was also performed in batch conditions after 24h of contact (Figure 7.a). Whereas lead(II) was the best retained cation by poly(MMA-*co*-EDMA), the adsorption of all cations by this resin was far less important than by NIP-D. Although, the ester functions could have been expected to interact with cations, all these observations tends to prove that the role of the iminodiacetic acid (IDA) ligand is crucial. This is in accordance with our earlier conclusions obtained by modelling the interactions of nickel with a VbIDA based IIP prepared by precipitation polymerization [34].

In order to study the imprinting effect, Amberlite® IRC 748 provided by Rohm and Haas was chosen as a second reference material because it contains IDA functions as chelating groups. It is based on a macroporous poly(styrene-*co*-divinylbenzene) matrix

with a high capacity (total exchange capacity (Na^+ form) ≥1.35 eq/L) and is commonly used to remove divalent metal cations without selectivity. Adsorption experiments were undertaken in competitive conditions as previously (with nickel, cobalt, zinc and lead). As expected, in such conditions this resin did not retain nickel preferentially: Q_{max}(Ni) = 315 µmol/g, Q_{max}(Zn) = 286 µmol/g, Q_{max}(Co) = 316 µmol/g and Q_{max}(Pb) = 66 µmol/g. Moreover, although these values were superior to those of IIPs, the difference was not so important. For instance, for nickel the ratio between maximum adsorption capacities of Amberlite® IRC 748 and IIP-D is only of 1.7. This evidences the good capacities of the prepared IIPs, although such kind of materials are usually expected to present low adsorption capacities.

Some major competing divalent cations that can be present in waters can affect the performances of IIPs in real samples. Therefore, the impact of calcium(II) and magnesium(II) on the IIPs and Amberlite® IRC 748 was examined in very competitive conditions: nickel, cobalt, zinc and lead introduced at 20 mg/L each and calcium and magnesium in large excess at 100 mg/L (Figure 7.b). Two conclusions can be drawn: (i) nickel adsorption capacities for all resins were not affected by the presence of these two cations, (ii) whereas magnesium and especially calcium were not retained by IIPs, the situation was inverted for Amberlite® IRC 748 which adsorbs a large amount of calcium. These results proved the efficiency of the imprinting process.

4. Conclusions

In this paper, we studied the impact of the porogen solvent on adsorption and selectivity properties of nickel ion-imprinted polymers. Two IIPs and their corresponding NIPs were synthesized in a bead format by inverse suspension copolymerization with VbIDA

as the functional complexing monomer. They were prepared with mixtures of DMSO and acetonitrile, 50/50 %v/v, for IIP-A/D and DMSO and 2-methoxyethanol, 50/50 %v/v, for IIP-M/D. The structure and properties of these polymers were compared with those of IIP-D previously prepared with pure DMSO as porogen [22]. Due to lower thermodynamic affinities of acetonitrile and 2-methoxyethanol with EDMA than DMSO, polymers prepared with these co-solvents were less porous than IIP-D and NIP-D. Nevertheless, their nickel adsorption properties and selectivity towards other divalent cations, namely Zn^{2+}, Co^{2+} and Pb^{2+}, were better. This proved that a decrease of the polymerization medium polarity improved the interactions between the chelating IDA groups and nickel. Moreover as a result of the stabilization of the ligand-metal complex during the polymerization process, the imprinting effect was significantly increased. Because of solubility concerns and of the need for the polymerization solvent to be non-miscible with mineral oil, we couldn't explore a large panel of solvents, especially less polar ones, although they might have better promoted the ligand-metal interactions. Nevertheless, the polarity of the studied solvents can also represent an advantage for the use of IIPs in aqueous medium.

In order to evaluate the impact of the crosslinker chemical structure on the IIPs properties, a copolymer of MMA and EDMA was prepared in the same conditions as NIP-D and compared to it. Both the adsorption of nickel and cross-selectivity were significantly better for NIP-D than for the poly(MMA-*co*-EDMA) proving the low binding properties of the methacrylic polymer matrix. Finally, adsorption of nickel by Amberlite® IRC 748, a commercial chelating resins with IDA groups, was measured in presence of the interfering Zn^{2+}, Co^{2+} and Pb^{2+} cations. For this resin, no selectivity for nickel was observed proving that selectivity of IIPs toward nickel is coming from an

imprinting effect and not from the choice of the chelating functions. Moreover, the nickel binding capacities of IIPs were around 55% of that of Amberlite® IRC 748. This result is particularly encouraging as IIPs usually suffer from low binding capacities. Finally, the impact of an excess of divalent calcium and magnesium ions was studied. These two major cations did not affect nickel adsorption and they were even not retained by the IIPs, contrary to Amberlite® IRC 748.

All of these results evidence (i) the need to choose a relevant porogen solvent, (ii) the importance of introducing some chelating agent in the imprinted polymers for ion recognition, (iii) the impact of the imprinting procedure on the selectivity results, (iv) the possibility to prepare IIPs with high binding capacities thanks to inverse suspension copolymerization.

References

[1] E. Denkhaus, K. Salnikow, Crit. Rev. Oncol. Hematol. 42 (2002) 35–56.
[2] K.S. Kasprzak, F.W. Sunderman, K. Salnikow, Mutat. Res. Mol. Mech. Mutagen. 533 (2003) 67–97.
[3] in:, IARC monographs on the evaluation of carcinogenic risks to humans. Chromium, nickel and welding. International Agency for Research on Cancer, Lyon, France, 1990.
[4] R. Beauvais, S. Alexandratos, React. Funct. Polym. 36 (1998) 113–123.
[5] V. Camel, Spectrochim. Acta Part B At. Spectrosc. 58 (2003) 1177–1233.
[6] T.P. Rao, S. Daniel, J.M. Gladis, TrAC Trends Anal. Chem. 23 (2004) 28–35.
[7] C. Branger, W. Meouche, A. Margaillan, React. Funct. Polym. 73 (2013) 859–875.
[8] A. Baghel, M. Boopathi, B. Singh, P. Pandey, T.H. Mahato, P.K. Gutch, K. Sekhar, Biosens. Bioelectron. 22 (2007) 3326–3334.
[9] D.K. Singh, S. Mishra, J. Sci. Ind. Res. 69 (2010) 767–772.
[10] T. Alizadeh, M.R. Ganjali, M. Zare, Anal. Chim. Acta 689 (2011) 52–59.
[11] S.-M. Ng, R. Narayanaswamy, Microchim. Acta 169 (2010) 303–311.
[12] H.-G. Wu, X.-J. Ju, R. Xie, Y.-M. Liu, J.-G. Deng, C.H. Niu, L.-Y. Chu, Polym. Adv. Technol. 22 (2011) 1389–1394.
[13] E. Birlik, A. Ersöz, E. AçIkkalp, A. Denizli, Ri. Say, J. Hazard. Mater. 140 (2007) 110–116.
[14] E.Ç. Demiralay, M. Andac, R. Say, G. Alsancak, A. Denizli, J. Appl. Polym. Sci. 117 (2010) 3704–3714.
[15] K. Laatikainen, D. Udomsap, H. Siren, H. Brisset, T. Sainio, C. Branger, Talanta 134 (2015) 538–545.
[16] M.T. Gokmen, F.E. Du Prez, Prog. Polym. Sci. 37 (2012) 365–405.
[17] O. Okay, Prog. Polym. Sci. 25 (2000) 711–779.
[18] J. Fu, L. Chen, J. Li, Z. Zhang, J. Mater. Chem. A 3 (2015) 13598–13627.
[19] M. Rammika, G. Darko, N. Torto, Water SA 38 (2012) 261–268.
[20] J.M. Gladis, T.P. Rao, Microchim. Acta 146 (2004) 251–258.
[21] B. Godlewska-Żyłkiewicz, B. Leśniewska, I. Wawreniuk, Talanta 83 (2010) 596–604.
[22] W. Meouche, C. Branger, I. Beurroies, R. Denoyel, A. Margaillan, Macromol. Rapid Commun. 33 (2012) 928–932.
[23] S. Dai, M.C. Burleigh, Y. Shin, C.C. Morrow, C.E. Barnes, Z. Xue, Angew. Chem. Int. Ed. 38 (1999) 1235–1239.
[24] K.S.W. Sing, D.H. Everett, R.A.W. Haul, L. Moscou, J. Rouquerol, T. Siemieniewska, Pure Appl. Chem. 57 (1985) 603–619.
[25] F.S. Macintyre, D.C. Sherrington, Macromolecules 37 (2004) 7628–7636.
[26] A.F.M. Barton, Chem. Commun. 75 (1975) 731–753.
[27] in:, CRC Handbook of Chemistry and Physics - 78th Edition, CRC Press, Inc., David R. Lide, 1997.
[28] J. Otero-Romaní, A. Moreda-Piñeiro, P. Bermejo-Barrera, A. Martin-Esteban, Microchem. J. 93 (2009) 225–231.
[29] M. Saraji, H. Yousefi, J. Hazard. Mater. 167 (2009) 1152–1157.
[30] A. Ersöz, R. Say, A. Denizli, Anal. Chim. Acta 502 (2004) 91–97.
[31] D.K. Singh, S. Mishra, Appl. Surf. Sci. 256 (2010) 7632–7637.

[32] M. Andaç, E. Özyapı, S. Şenel, R. Say, A. Denizli, Ind. Eng. Chem. Res. 45 (2006) 1780–1786.
[33] Y. Liu, Z. Liu, J. Dai, J. Gao, J. Xie, Y. Yan, Chin. J. Chem. 29 (2011) 387–398.
[34] V. Lenoble, W. Meouche, K. Laatikainen, C. Garnier, H. Brisset, A. Margaillan, C. Branger, J. Colloid Interface Sci. 448 (2015) 473–481.

Figures and tables captions

Table 1: Characteristics of IIPs and NIPs: porogen solvent, porous properties, maximum nickel binding capacities and imprinting factors
Table 2: Rate constants (k_1 and k_2) and correlation coefficients
Table 3: Maximum adsorption capacities (µmol/g), selectivity coefficients and relative selectivity coefficients determined by batch after 24h at pH 7.5

Scheme 1: VbIDA structure

Figure 1: FTIR spectra (KBr pellets, transmittance) of (a) NIP-D, (b) NIP-A/D, (c) NIP-M/D, (d) unleached IIP-D, (e) unleached IIP-A/D, (f) unleached IIP-M/D, (g) leached IIP-D, (h) leached IIP-A/D and (i) leached IIP-M/D
Figure 2: SEM pictures of IIP-A/D (a), NIP-A/D (b), IIP-M/D (c) and NIP-M/D (d)
Figure 3: Nitrogen adsorption/desorption isotherms of IIP-D, NIP-D, IIP-A/D (a), NIP-A/D (b), IIP-M/D (c) and NIP-M/D (d) (figure 25 thèse)
Figure 4: Isotherms of nickel(II) adsorption for IIP-A/D (a), NIP-A/D (b), IIP-M/D (c) and NIP-M/D (d) at pH 7.5
Figure 5: Kinetic study of the complexation of nickel(II), cobalt(II), zinc(II) and lead(II) at pH 7.5
Figure 6: Nitrogen adsorption/desorption isotherms of NIP-A/D and poly(MMA-co-EDMA) (figure 30 thèse)
Figure 7: (a) fig.32 thèse and (b) fig.33 thèse

Table 1: Characteristics of IIPs and NIPs: porogen solvent, porous properties, maximum nickel binding capacities and imprinting factors

	IIP-D	NIP-D	IIP-A/D	NIP-A/D	IIP-M/D	NIP-M/D
Porogen solvent	DMSO		Acetonitrile/DMSO (50/50, v/v)		2-Methoxyethanol/DMSO (50/50, v/v)	
S_{BET} ($m^2.g^{-1}$)	275	380	134	181	177	457
Average pore diameter (nm)	5.4	10.6	Large distribution	Large distribution	Large distribution	Large distribution
Total porous volume ($cm^3.g^{-1}$)	0.25	0.62	0.15	0.27	0.17	0.67
Microporous volume ($cm^3.g^{-1}$)	0.05	0.06	0.02	0	0.02	0.08
Mesoporous volume ($cm^3.g^{-1}$)	0.20	0.56	0.13	0.27	0.15	0.59
Hysteresis type	H2	H1	H2	H2	H2	H1
Q_{max} (µmol/g)	242±12	139±7	408±20	147±7	381±19	151±7
Q_{max} (mg/g)	14.2±0.7	8.1±0.4	23.9±1.1	8.6±0.4	22.4±1.1	8.9±0.4
Imprinting factor	1.74	-	2.77	-	2.52	-

Table 2: Rate constants (k_1 and k_2) and correlation coefficients R^2 for IIPs and NIPs

IIPs	**Metal**	**First order model**		**Second order model**			$k_{1,Ni} / k_{1,Metal}$
		k_1(min^{-1})	$R_1{}^2$	q_e	k_2 (g.mg^{-1}.min^{-1})	$R_2{}^2$	
IIP-D	Ni	0.0044	0.988	14.49	-0.0003	0.773	/
	Zn	0.0035	0.998	2.22	-0.0012	0.650	1.25
	Co	0.0025	0.999	1.09	-0.0010	0.573	1.75
	Pb	0.0509	0.911	5.03	-0.0157	0.12	/
IIP-A/D	Ni	0.0037	0.992	12.32	-0.0002	0.639	/
	Zn	0.0026	0.999	2.59	-0.0002	0.374	1.42
	Co	0.0022	0.999	0.12	-0.0005	0.354	1.68
	Pb	0.0262	0.881	5.14	-0.0050	0.214	/
IIP-M/D	Ni	0.0037	0.992	15.85	-0.0002	0.663	/
	Zn	0.0027	0.999	1.05	-0.0009	0.529	1.37
	Co	0.0017	0.999	0.76	-0.0001	0.126	2.17
	Pb	0.0390	0.179	7.15	-0.0101	0.005	/

NIPs	**Metal**	**First order model**		**Second order model**			$k_{1,Ni} / k_{1,Metal}$
		k_1 (min^{-1})	$R_1{}^2$	q_e	k_2 (g.mg^{-1}.min^{-1})	$R_2{}^2$	
NIP-D	Ni	0.0031	0.997	2.68	-0.013	0.929	/
	Zn	0.0032	0.999	0.67	-0.005	0.953	0.96
	Co	0.0024	0.999	0.42	-0.003	0.732	1.29
	Pb	0.0530	0.941	5.31	-0.013	0.106	/
NIP-A/D	Ni	0.0012	0.999	0.09	-0.0012	0.738	/
	Zn	0.0012	0.999	0.09	-0.0005	0.294	1.00
	Co	-0.0007	1	-0.04	-0.0006	0.354	/
	Pb	0.0258	0.971	7.70	-0.0080	0.470	/
NIP-M/D	Ni	0.0015	0.999	0.59	-0.0004	0.759	/
	Zn	0.0014	0.999	0.43	-0.0001	0.529	1.07
	Co	0.0007	1	0.08	-0.0001	0.568	2.14
	Pb	-0.107	0.801	-0.79	-1.0237	0.795	/

Table 3: Maximum adsorption capacities (µmol/g), selectivity coefficients and relative selectivity coefficients determined by batch after 24h. T = 25ºC, I_s = 0.1 mol/L (nitrate media), pH = 7.5 in the equilibrium, and c_{metals} = 20 mg/L.

Polymer	Cation	Q_{max}IIP (µmol/g)	Q_{max}NIP (µmol/g)	k_{IIP}	k_{NIP}	k'
IIP-D and NIP-D	Ni	183.9	123.1	-	-	-
	Zn	101.2	85.5	2.55	1.48	1.73
	Co	89.2	80.6	3.73	1.92	1.91
	Pb	77.0	76.7	0.29	0.13	2.17
IIP-A/D and NIP-A/D	Ni	169.9	49.3	-	-	-
	Zn	92.4	41.5	2.43	1.07	2.27
	Co	63.8	28.1	10.94	1.93	5.66
	Pb	63.8	81.2	0.54	0.02	21.95
IIP-M/D and NIP-M/D	Ni	174.3	67.3	-	-	-
	Zn	75.8	50.3	3.22	1.21	2.65
	Co	64.4	44.9	4.81	1.63	2.95
	Pb	83.7	72.0	0.16	0.03	6.13

Scheme 1:VbIDA structure

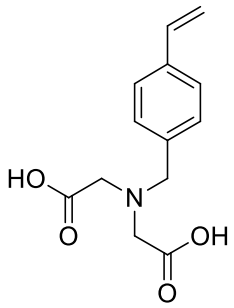

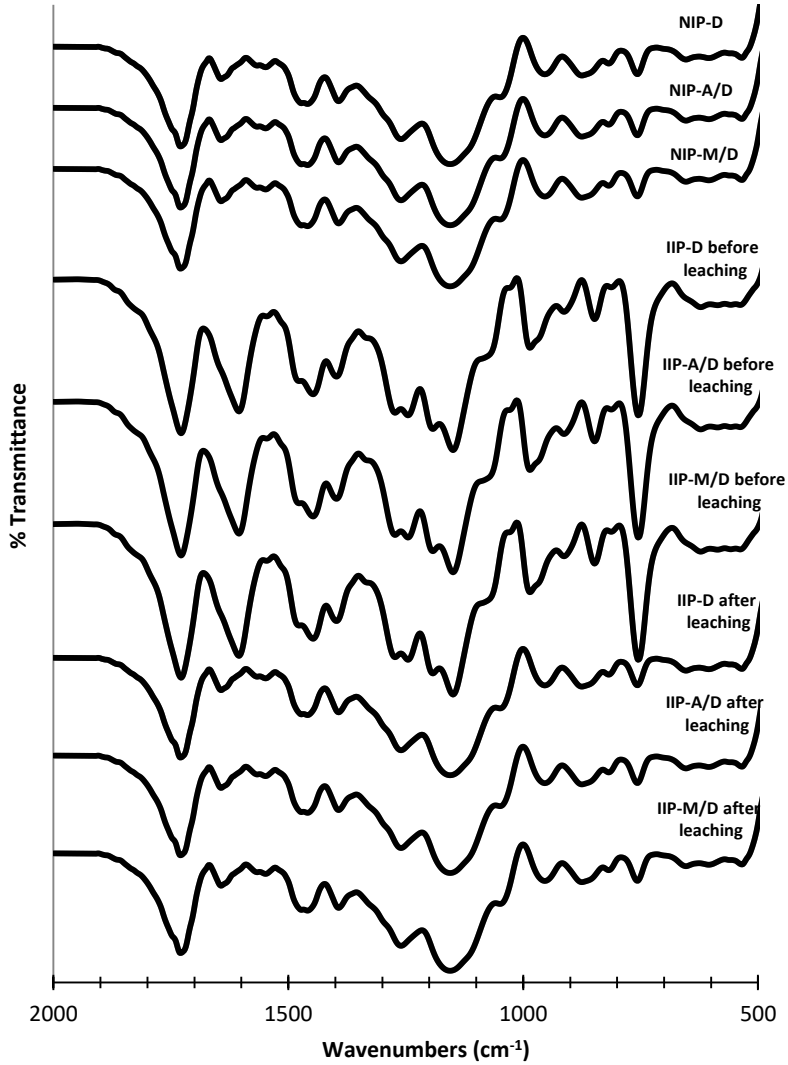
NIP-D
NIP-A/D
NIP-M/D
IIP-D before leaching
IIP-A/D before leaching
IIP-M/D before leaching
IIP-D after leaching
IIP-A/D after leaching
IIP-M/D after leaching
% Transmittance
2000
1500
1000
500
Wavenumbers (cm-1)

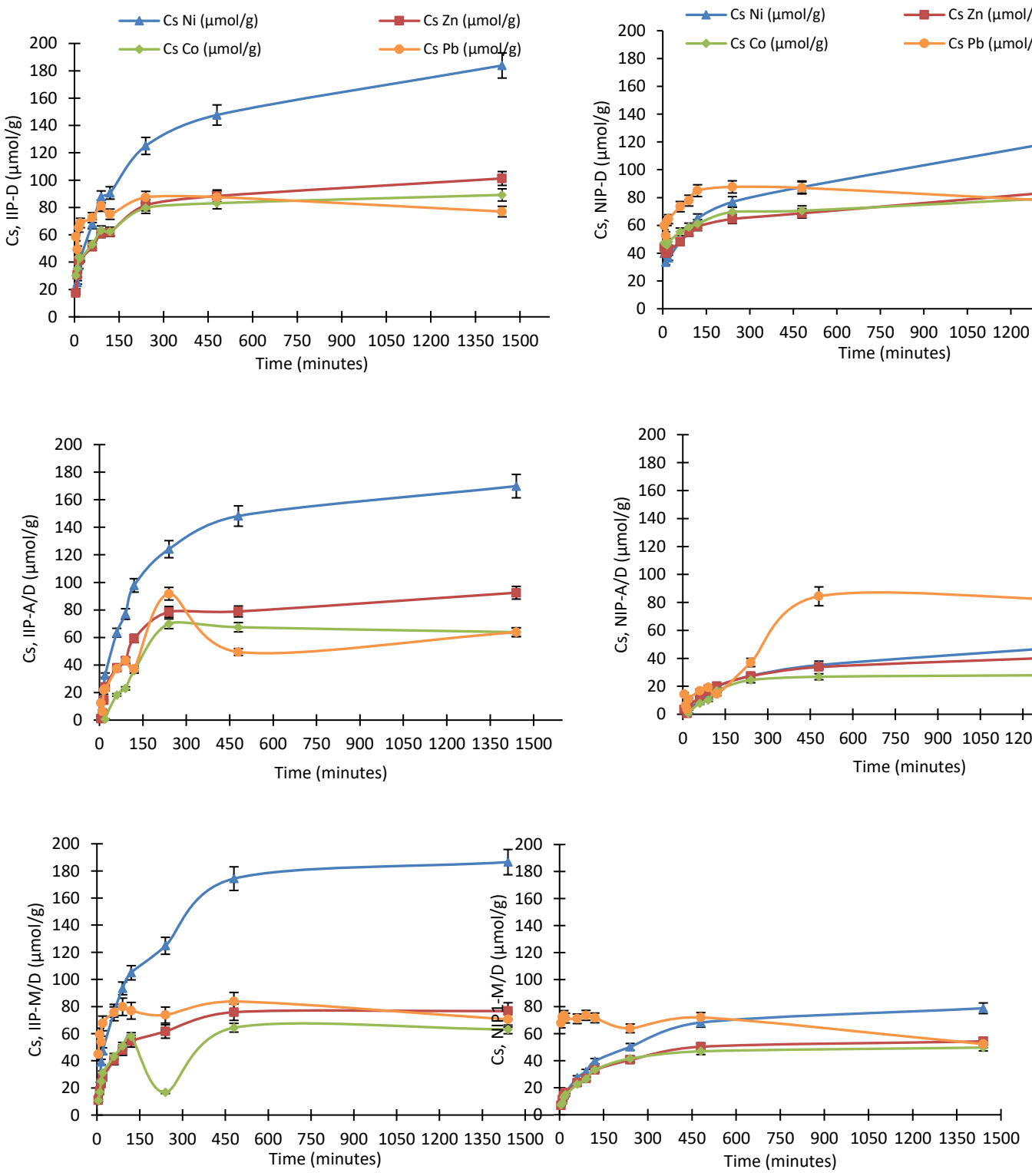

Figure 5: Kinetic study of the complexation of nickel(II), cobalt(II), zinc(II) and lead(II) at pH 7.5

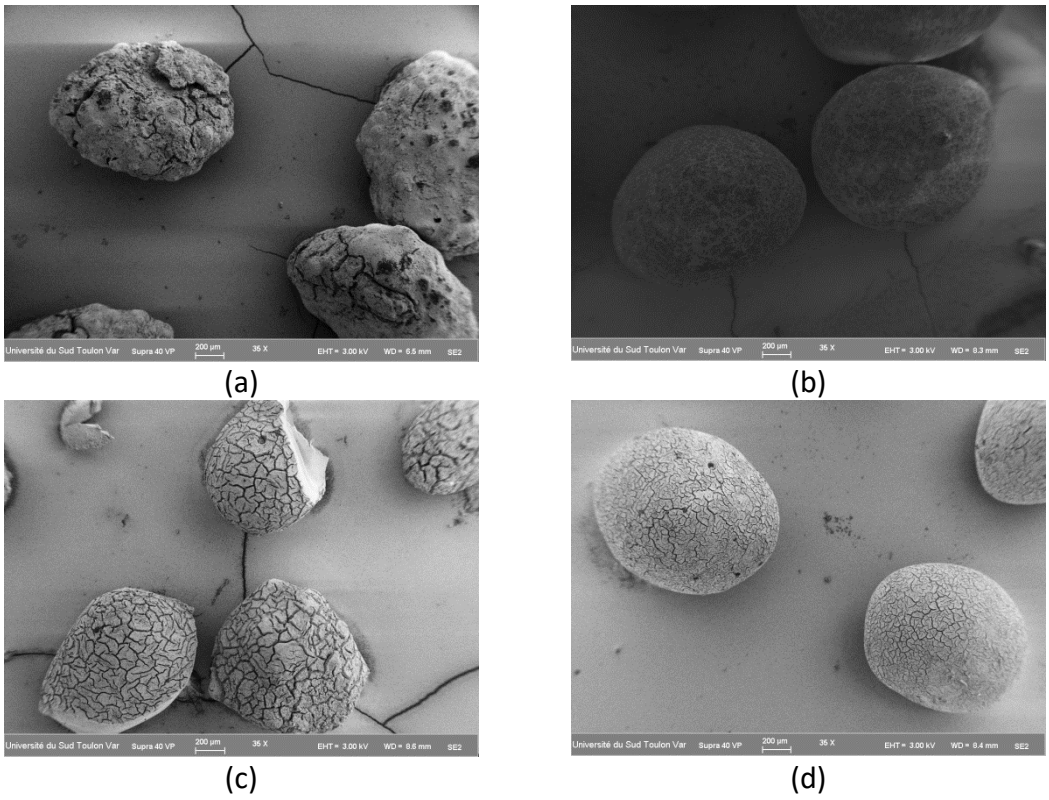

Figure 2: SEM pictures of IIP-A/D (a), NIP-A/D (b), IIP-M/D (c) and NIP-M/D (d)

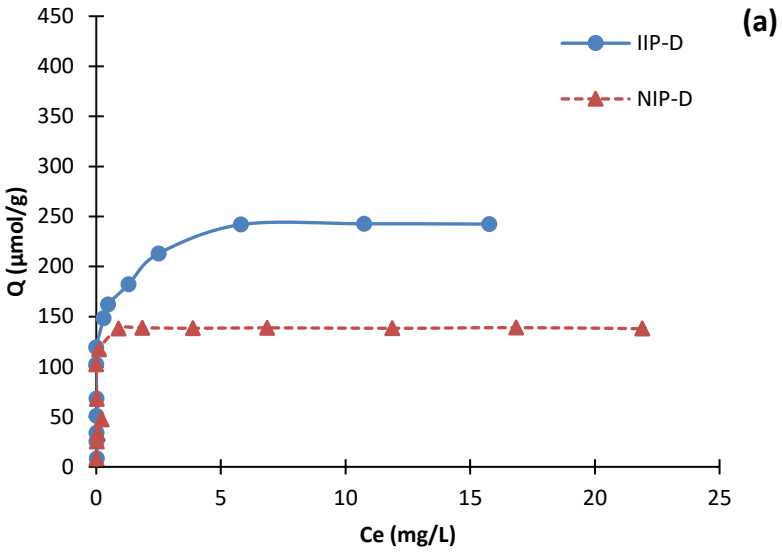
(a)
IIP-D
NIP-D
Q (µmol/g)
Ce (mg/L)
0
50
100
150
200
250
300
350
400
450
0
5
10
15
20
25

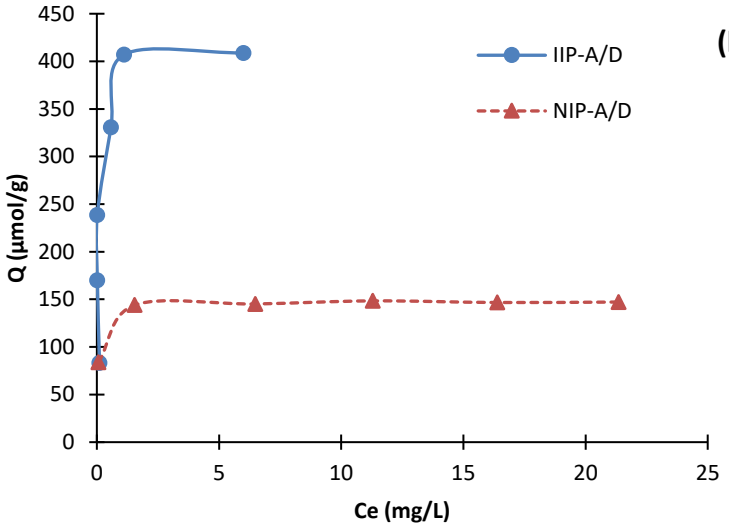
(b)
IIP-A/D
NIP-A/D
Q (µmol/g)
Ce (mg/L)
0
50
100
150
200
250
300
350
400
450
0
5
10
15
20
25

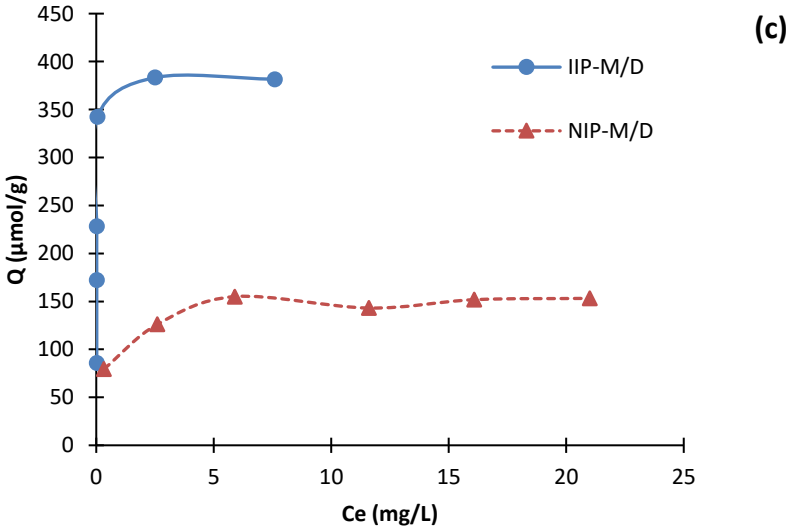
(c)
IIP-M/D
NIP-M/D
Q (µmol/g)
Ce (mg/L)
0
50
100
150
200
250
300
350
400
450
0
5
10
15
20
25

Figure 4: Isotherms of nickel(II) adsorption for IIP-A/D (a), NIP-A/D (b), IIP-M/D (c) and NIP-M/D (d) at pH 7.5

Figure 7: